doi:10.1016/S0022-2836(03)00631-4 J. Mol. Biol. (2003) 330, 651–656

JMB

Available online at www.sciencedirect.com

SCIENCE DIRECT®

COMMUNICATION

Structural Plasticity and the Evolution of Antibody Affinity and Specificity

Jun Yin[1,2], Albert E. Beuscher IV[3], Scott E. Andryski[1,2] Raymond C. Stevens[3]* and Peter G. Schultz[2]*

[1]*Department of Chemistry University of California at Berkeley, Berkeley, CA 94720 USA*

[2]*Department of Chemistry and The Skaggs Institute of Chemical Biology, The Scripps Research Institute, 10550 North Torrey Pines Road La Jolla, CA 92037, USA*

[3]*Department of Molecular Biology and The Skaggs Institute of Chemical Biology The Scripps Research Institute 10550 North Torrey Pines Road La Jolla, CA 92037, USA*

**Corresponding authors*

The germline precursor to the ferrochelatase antibody 7G12 was found to bind the polyether jeffamine in addition to its cognate hapten *N*-methylmesoporphyrin. A comparison of the X-ray crystal structures of the ligand-free germline Fab and its complex with either hapten or jeffamine reveals that the germline antibody undergoes significant conformational changes upon the binding of these two structurally distinct ligands, which lead to increased antibody-ligand complementarity. The five somatic mutations introduced during affinity maturation lead to enhanced binding affinity for hapten and a loss in affinity for jeffamine. Moreover, a comparison of the crystal structures of the germline and affinity-matured antibodies reveals that somatic mutations not only fix the optimal binding site conformation for the hapten, but also introduce interactions that interfere with the binding of non-hapten molecules. The structural plasticity of this germline antibody and the structural effects of the somatic mutations that result in enhanced affinity and specificity for hapten likely represent general mechanisms used by the immune response, and perhaps primitive proteins, to evolve high affinity, selective receptors for so many distinct chemical structures.

Keywords: jeffamine; structural plasticity; germline antibody; somatic mutation; affinity maturation

The evolution of antibody binding affinity and specificity by the immune system involves genetic recombination, random mutation and affinity-based selection, which in many aspects parallel those mechanisms involved in the natural evolution of enzymes.[1] After the combinatorial assembly of the antibody gene, the germline antibody undergoes affinity maturation during which somatic mutations are introduced into the antibody variable region, leading to increased antibody binding affinity and specificity for the antigen.[2] Detailed structural studies of affinity-matured catalytic antibodies and their germline precursors have provided important insights into the evolution of both binding energy and catalysis in biological systems. In the majority of cases studied to date, the germline antibodies undergo significant loop rearrangements and side-chain conformational changes upon hapten binding, whereas the affinity-matured antibodies adopt a "lock-and-key" mode of binding.[3–6] These studies led to the hypothesis that the structural plasticity associated with the germline antibody, like sequence diversity, plays a critical role in the ability of the immune system to generate antibodies with so many distinct specificities. Subsequent somatic mutations pre-organize the antibody combining site for high antigen binding affinity and specificity in the affinity-matured antibody.[1] Here we provide the first clear structural evidence for this hypothesis in which a germline antibody binds two different ligands with two distinct active site conformations and evolves affinity and specificity for its cognate antigen by somatic mutations that fix one optimal active site conformation.

Antibody 7G12 was raised against *N*-methylmesoporphyrin (NMP), a mimic of the strained porphyrin substrate, and catalyzes mesoporphyrin metallation by Cu^{2+} and Zn^{2+} with a catalytic efficiency for Zn^{2+} incorporation approaching that of

Abbreviations used: CDR, complementarity determining region; Fab, fragment, antigen binding; NMP, *N*-methylmesoporphyrin IX; MP, mesoporphyrin IX.

E-mail addresses of the corresponding authors: stevens@scripps.edu; schultz@scripps.edu

Table 1. Data collection and refinement statistics

Space group	$P2_1$
Unit cell dimensions	
a (Å)	70.6
b (Å)	64.7
c (Å)	93.4
α (deg.)	90
β (deg.)	92.6
γ (deg.)	90
Refinement resolution (Å)	20.0–1.7
Observations (n)	97,524
Unique reflections (*n*)	44,964
R_{sym} (*I*) (%)[a]	3.4
R_{cryst} (%)[b]	21.7
R_{free} (%)[c]	24.1
Completeness to the refined resolution (%)	91.2

[a] $R_{sym} = 100 \times \sum_h \sum_i I_{h,i} - I_h / \sum_h \sum_i I_{h,i}$ for the intensity *I* of *i* observations of reflection *h*. I_h is the mean intensity of the reflection.

[b] $R_{cryst} = 100 \times \sum |F_{obs} - F_{calc}| / \sum |F_{obs}|$, where F_{obs} and F_{calc} are the observed and calculated structure factors, respectively.

[c] R_{free} is the same as *R* factor, but is calculated from the 10% of the reflection data excluded from refinement.

the natural enzyme ferrochelatase.[7] A total of five somatic mutations accumulated during the affinity maturation of the germline precursor antibody to 7G12. Three somatic mutations, Ala32^{L}Pro, Arg50^{H}Met and Ser97^{H}Met, are in close vicinity to the antibody combining site, and the other two, Ser14^{L}Thr and Ser76^{H}Asn, are in peripheral regions, 29 Å and 21 Å away from the bound hapten, respectively.[8] The crystal structure of the unliganded and hapten NMP complexed antigen binding fragments (Fabs) of the germline and affinity-matured antibodies have been solved.[6,8]

When jeffamine ($CH_3OCH_2CH_2O(CH(CH_3)CH_2O)_nCH_2CH(NH_2)CH_3$, $n \sim 8$) was used as an additive (1% v/v) during crystallization trials for the 7G12 germline Fab, hexagonal antibody crystals were readily obtained at 25 °C and gave X-ray diffraction to 1.7 Å resolution. The crystal structure of the germline Fab was solved by molecular replacement (Table 1); in the $F_o - F_c$ omit map we observed well-defined electron density in the antibody combining site which could not be accounted for by the side-chains or the backbone of the Fab molecule. Seven units of the isopropoxy group of the jeffamine molecule could be modeled into the antibody combining site and fit well into the U-shaped, long stretch of electron density (Figure 1).

Binding of jeffamine to the 7G12 germline Fab was confirmed by surface plasmon resonance; the dissociation constant (K_d) of the germline Fab–jeffamine complex was determined to be 11.2 μM and the binding can be inhibited by addition of NMP. However, the binding between the affinity-matured 7G12 Fab and jeffamine is very weak with a K_d at least 20-fold higher than that of the germline Fab (Table 2). For comparison, the K_d for the germline Fab–NMP complex is 1.96 μM and the K_d for the affinity-matured 7G12 Fab–NMP complex is 20.7 nM.[6] Thus the germline antibody of 7G12 is capable of binding two structurally distinct ligands, whereas the affinity-matured antibody binds selectively to the hapten NMP with high affinity. The heavy chain variable region of

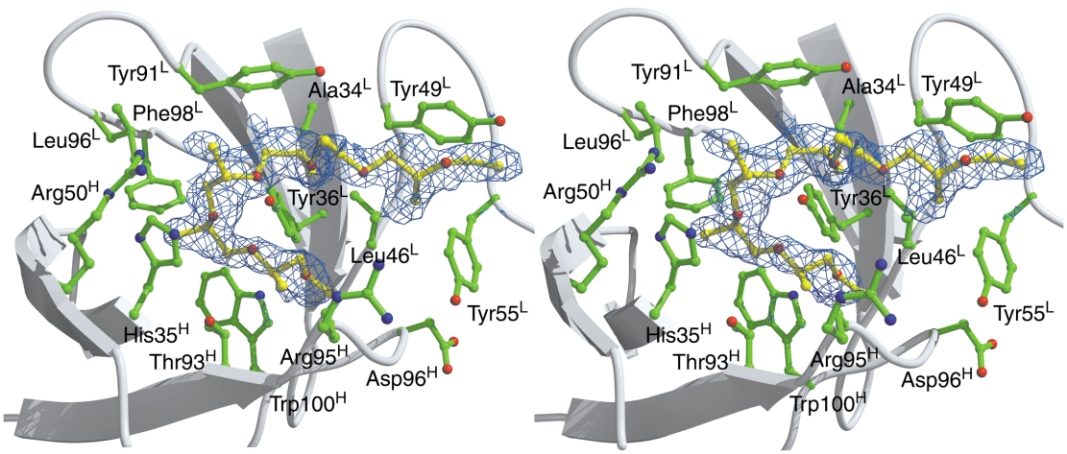

Figure 1. Stereo diagram of $F_o - F_c$ electron density maps contoured at 2.0σ for the jeffamine molecule (colored in yellow) bound with the germline Fab. Residues in the antibody combining site making important packing interactions with jeffamine are also shown. This Figure was prepared with BOBSCRIPT[16] and Raster3D.[17] The Fab fragment of 7G12 germline antibody was cloned previously[8] and was expressed from *Escherichia coli*. 25F2 cells and purified as described.[6] The complex of 7G12 Fab and jeffamine was crystallized by hanging drop methods from 25%(w/v) PEG 2000 monomethylether, 165 mM ammonium sulfate, 1.0%(v/v) jeffamine, 100 mM Tris (pH 6.6) at 25 °C. Data sets were collected in house with a FRD generator and a RAXISIV^{2+} detector. Data were processed with DENZO and SCALEPACK.[18] The structure was determined by molecular replacement techniques using the structure of 7G12 Fab–NMP complex from PDB entry 3FCT[8] with the program EPMR.[19] Mutation of the molecular replacement model and rebuilding was done using the program O.[20] Refinement was carried out using positional, simulated annealing and torsional refinement in CNS,[21] with NCS restraints turned on and bulk solvent corrections applied between 20.0 Å and 6.0 Å.

Table 2. Binding of 7G12 Fab, germline Fab and the mutants to jeffamine and NMP

Fab	k_{on} (jeffamine) (10^3 $M^{-1}s^{-1}$)	k_{off} (jeffamine) (10^{-2} s^{-1})	K_d (jeffamine) (10^{-6} M)	ΔG (jeffamine) (kcal/mol)	K_d (NMP) (10^{-6} M)	ΔG (NMP) (kcal/mol)
7G12	–	–	≥200	≥ −5.04	0.0207	−10.5
Germline	0.556	0.623	11.2	−6.75	1.96	−7.78
Germline mutants						
$Ala32^{L}Pro$	0.716	0.752	10.5	−6.79	0.808	−8.31
$Arg50^{H}Met$	0.419	0.843	20.1	−6.41	0.595	−8.49
$Ser97^{H}Met$	–	–	≥200	≥ −5.04	0.398	−8.73
7G12 mutants						
$Pro32^{L}Ala$	–	–	≥200	≥ −5.04	0.151	−9.30
$Met50^{H}Arg$	–	–	≥200	≥ −5.04	0.295	−8.91
$Met97^{H}Ser$	0.510	0.801	15.7	−6.55	0.373	−8.77
Mixed mutants						
$_{Germline}L/_{7G12}H$	–	–	≥200	≥ −5.04	0.203	−9.13
$_{7G12}L/_{germline}H$	0.388	0.745	19.2	−6.43	1.02	−8.17

In the "germline mutants", each somatic mutation was introduced individually into the germline antibody. In the "7G12 mutants", each residue in the affinity matured antibody derived from somatic mutation was switched back to its germline identity. In the "mixed mutants" the light and the heavy chains of the germline and the affinity matured antibodies are crosscombined. The binding properties (K_d and k_{off}) of 7G12 Fab, germline Fab and all the mutants with jeffamine were measured by surface plasmon resonance on a Biacore 3000 biosensor following published methods.[6] Bovine serum albumin was conjugated with jeffamine and was immobilized on a research grade CM5 sensor chip (Biacore). The dissociation constant K_d was measured under equilibrium conditions and the dissociation rate constant was measured under kinetic conditions. The association constant (k_{on}) was calculated with the equation $k_{on} = k_{off}/K_d$. ΔG was calculated with equation $\Delta G = 2.303RT \log K_d$. The binding data of the germline Fab, affinity matured Fab and various mutants with the hapten NMP are from Yin *et al.*[6]

7G12 germline antibody derives from the combination of V186.2 of J558 subfamily with DSP2.2 and J_H3 gene segments.[9] Interestingly, a number of antibodies encoded by V_H genes from the J558 family were found to be polyspecific, binding a number of structurally distinct ligands.[10–13]

The crystal structure of the germline Fab–jeffamine complex reveals that five isopropoxy units of the jeffamine molecule fold into a U-shaped conformation and are deeply embedded in the antibody combining site consisting of mainly hydrophobic residues including $Tyr36^{L}$, $Leu46^{L}$, $Tyr49^{L}$, $Tyr91^{L}$, $Leu96^{L}$ and $Phe98^{L}$ from the light chain and $Thr93^{H}$ and $Trp100^{H}$ from the heavy chain (Figures 1 and 2(A)). A hydrogen bond is formed between O6 of jeffamine and the indole $N^{\varepsilon 1}$ of $Trp100^{H}$ (2.8 Å). $His35^{H}$ and $Arg95^{H}$ also pack on the poly(isopropoxy) backbone of the jeffamine molecule. Superposition of the unliganded germline Fab with either the germline

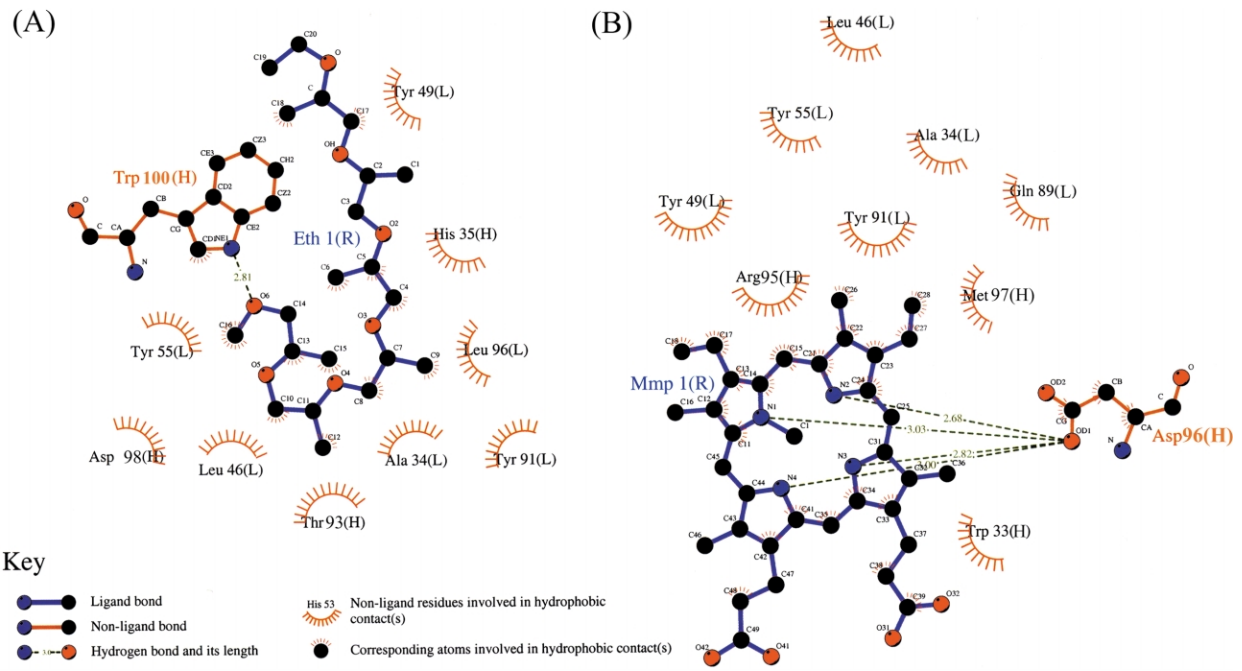

Figure 2. Comparison of the specific interactions of the germline Fab with jeffamine (A) and NMP (B). NMP and jeffamine are drawn in ball and stick. This Figure was prepared with Ligplot.[22]

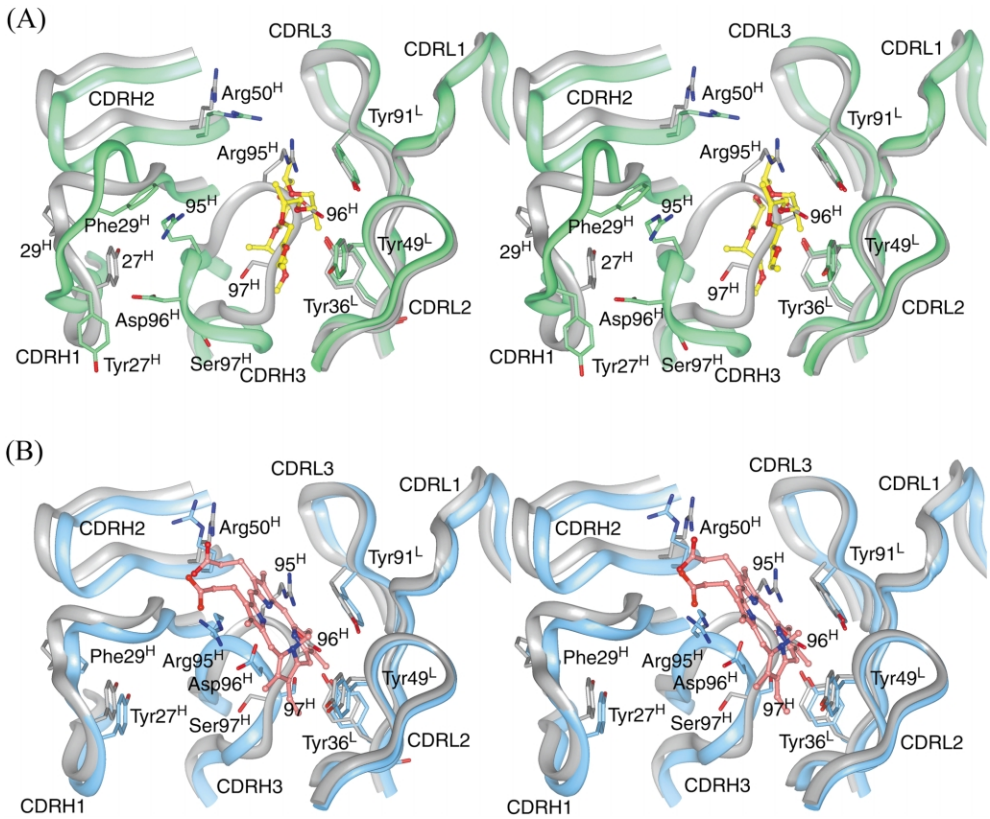

Figure 3. (A) Overlay of the crystal structures of the unliganded germline Fab (gray) and the germline Fab–jeffamine complex (green). The jeffamine molecule is drawn in yellow and in ball and stick. (B) Overlay of the crystal structures of the unliganded germline Fab (gray) and the germline Fab–hapten NMP complex (blue). NMP molecule is drawn in pink and in ball and stick.

Fab–jeffamine complex or the germline Fab–NMP complex[6] reveals that the heavy chain complementarity determining region (CDR) loops undergo significant rearrangement upon the binding of NMP and even larger changes upon the binding of jeffamine (Figure 3). In contrast, the conformation of the light chain CDRs does not change significantly upon the binding of the ligands. The C^{α} of $Asp96^{H}$ of CDRH3 moves 10.9 Å away from the light chain in order to accommodate jeffamine. This forces a conformational change of CDRH1 to avoid steric clashes between the side-chain of $Tyr27^{H}$ and the carboxyl group of $Asp96^{H}$ (Figure 3(A)). As a result of antibody combining site reorganization, two different sets of residues are used by the germline antibody to interact with NMP and jeffamine (Figure 2). For an example, $Asp96^{H}$ plays a crucial role in binding NMP by orienting the carboxyl oxygen toward the center of NMP and forming multiple hydrogen bonds with the pyrrole nitrogen atoms of NMP. However, in the germline Fab–jeffamine complex this residue is pointing away from the antibody combining site and does not interact with the jeffamine ligand due to the CDR loop rearrangements. Instead, residues $His35^{H}$, $Arg50^{H}$, $Asp98^{H}$ and $Trp100^{H}$ are in close vicinity to the jeffamine ligand and contribute to binding.

The structural plasticity of the germline antibody that allows the antibody combining site to bind structurally distinct ligands is also evident in a comparison of the electrostatic surface of the same antibody combining site before and after binding of ligands. As shown in Figure 4, the ligand-free germline Fab has a shallow combining site, whereas the binding of both NMP and jeffamine induce structural reorganizations that result in the formation of deep cavities to accommodate the ligands. However, the shape and the charge distribution of the cavities formed are quite different for the two ligands. The binding of NMP leads to a curved narrow cavity that is complementary in shape to the distorted porphyrin ring of NMP. The net negative charges distributed inside the binding cavity are complementary to the positively charged NMP pyrrole nitrogen. In contrast, the binding of jeffamine induces the formation of a deep cylindrical cavity that binds a U-shaped conformation of the jeffamine molecule through hydrophobic packing and hydrogen bonding with a mainly neutral protein surface surrounding the ligand. These findings reinforce the notion that the conformational plasticity of the germline antibody gives rise to polyspecificity and plays a key role in expanding the germline binding repertoire.

To evaluate the effects of the somatic mutations on the binding of jeffamine and hapten, we characterized the binding affinities of various somatic

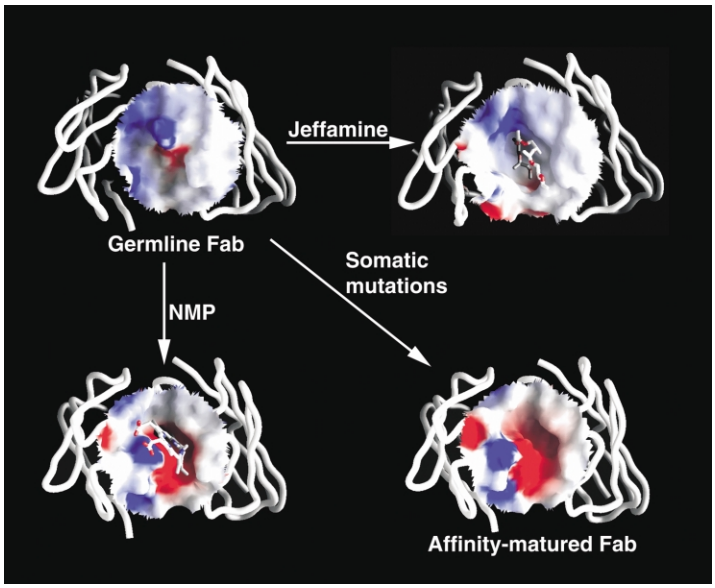

Figure 4. Conformational change of the germline antibody combining site upon the binding of structurally distinct ligands NMP or jeffamine or upon the incorporation of somatic mutations during affinity maturation. The red and blue colors on the surface of the antibody combining site correspond to negative and positive surface potential, respectively. This Figure was prepared with GRASP.[23]

mutants in the context of both the germline and the affinity-matured Fab (Table 2). The somatic mutation Ser97^{H}Met appears to be the major determinant: this mutation in the germline Fab eliminates the binding of jeffamine, while the reverse Met97^{H}Ser mutation in the affinity-matured antibody restores binding affinity to jeffamine. A comparison of the structures of the germline Fab–jeffamine complex and the ligand-free affinity-matured Fab[6] reveals that the Ser97^{H}Met somatic mutation in the germline Fab locks the conformation of CDRH3 through packing interactions between the newly introduced methionine side-chain and the residues of Tyr36^{L}, Gln89^{L}, Leu96^{L} and Phe98^{L} (Figure 5). The side-chain of Met97^{H} also interferes with the binding of jeffamine by occupying the position that C10–C14 of jeffamine would bind in the germline Fab (Figure 5). However, the same somatic mutation increases the binding affinity of hapten NMP to the germline Fab by fivefold (the Ser97^{H}Met germline mutant–NMP complex has a K_d of 0.398 μM[6]).

Thus the germline precursor to 7G12 has an intrinsic structural flexibility in the heavy chain CDR loops and the binding of the hapten or non-hapten ligands induces CDR loop rearrangements that increase complementarity between the antibody and those ligands. The somatic mutations acquired by the affinity-matured antibody act to both fix the conformation of the CDR loops for specific hapten binding, as well as introduce side-chains that interfere with the binding of non-hapten ligands so as to render the affinity-matured antibody highly specific. These and other structural studies of the germline and affinity-matured antibodies[3–6] have shown that the early theories proposed by Haurowitz and others to explain the basis for antibody specificity, i.e. antibody combining sites, like the human hand, can be molded to different ligands,[14,15] are to a large degree correct. Somatic mutations, rather than multiple stable

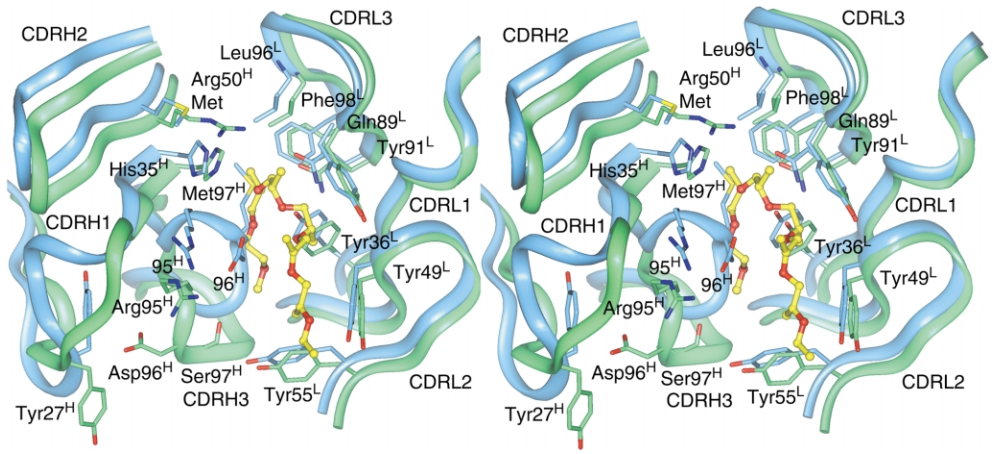

Figure 5. Overlay of the germline Fab–jeffamine complex (green) and the unliganded affinity-matured 7G12 Fab (blue). The jeffamine molecule is drawn in yellow and in ball and stick.

folds, serve to lock the preferred binding conformation. Thus the binding potential of the immune system appears to be determined by both sequence and conformational diversity. Given the similarities between the evolution of antibodies and enzymes, one can hypothesize that structural plasticity may have also allowed a limited number of primitive proteins to achieve a highly diverse binding and catalytic repertoire. The optimized active site structures for a given function were than fixed by natural mutation and selection processes.

Coordinates

The coordinates and structure factor amplitudes for 7G12 germline Fab–jeffamine complex have been deposited with the Protein Data Bank under accession code 1NGX.

Acknowledgements

This work was supported by National Institutes of Health grant GM56528. This is paper 15390-CH of The Scripps Research Institute.

References

1. Schultz, P. G., Yin, J. & Lerner, R. A. (2002). The chemistry of the antibody molecule. *Angew. Chem. Int. Ed.* **41**, 4427–4437.
2. Tonegawa, S. (1983). Somatic generation of antibody diversity. *Nature*, **302**, 575–581.
3. Wedemayer, G. J., Patten, P. A., Wang, L. H., Schultz, P. G. & Stevens, R. C. (1997). Structural insights into the evolution of an antibody combining site. *Science*, **276**, 1665–1669.
4. Mundorff, E. C., Hanson, M. A., Varvak, A., Ulrich, H., Schultz, P. G. & Stevens, R. C. (2000). Conformational effects in biological catalysis: an antibody-catalyzed oxy-cope rearrangement. *Biochemistry,* **39**, 627–632.
5. Yin, J., Mundorff, E. C., Yang, P. L., Wendt, K. U., Hanway, D., Stevens, R. C. & Schultz, P. G. (2001). A comparative analysis of the immunological evolution of antibody 28B4. *Biochemistry,* **40**, 10764–10773.
6. Yin, J., Andryski, S., Beuscher, A. E., IV, Stevens, R. C. & Schultz, P. G. (2003). Structural evidence for substrate strain in antibody catalysis. *Proc. Natl Acad. Sci. USA*, **100**, 851–861.
7. Cochran, A. G. & Schultz, P. G. (1990). Antibody-catalyzed porphyrin metallation. *Science*, **249**, 781–783.
8. Romesberg, F. E., Santarsiero, B. D., Spiller, B., Yin, J., Barnes, D., Schultz, P. G. & Stevens, R. C. (1998). Structural and kinetic evidence for strain in biological catalysis. *Biochemistry,* **37**, 14404–14409.
9. Kabat, E. A., Wu, T. T., Perry, H. M., Gottesman, K. S. & Foeller, C. (1991). *Sequences of Proteins of Immunological Interests*, 5th edit., US Department of Health and Human Services, National Institute of Health, Bethesda, MD.
10. Conger, J. D., Sage, H. J. & Corley, R. B. (1992). Correlation of antibody multireactivity with variable region primary structure among murine anti-erythrocyte autoantibodies. *Eur. J. Immunol.* **22**, 783–790.
11. Kasturi, K. N., Yio, X. Y. & Bona, C. A. (1994). Molecular characterization of J558 genes encoding tight-skin mouse autoantibodies. *Proc. Natl Acad. Sci. USA*, **91**, 8067–8071.
12. Lipsanen, V., Walter, B., Emara, M., Siminovitch, K., Lam, J. & Kaushik, A. (1997). Restricted CDR3 length of the heavy chain is characteristic of six randomly isolated disease-associated V_H J558 IgM autoantibodies in lupus prone metheaten mice. *Inter. Immunol.* **9**, 655–664.
13. Shimoda, M., Inoue, Y., Azuma, N. & Kanno, C. (1999). Natural polyreactive immunoglobulin A antibodies produced in mouse Peyer's patches. *Immunology*, **97**, 9–17.
14. Breinl, F. & Haurowitz, F. (1930). Chemische untersuchung des präzipitates aus hämoglobin und anti-hämoglobin-serum und bemerkungen über die natur der antikörper. *Z. Physiol. Chem.* **192**, 45–57.
15. Pauling, L. (1940). A theory of the structure and process of formation of antibodies. *J. Am. Chem. Soc.* **62**, 2643–2657.
16. Esnouf, R. M. (1997). An extensively modified version of MolScript that includes greatly enhanced coloring capabilities. *J. Mol. Graph. Model.* **15**, 132–138.
17. Merritt, E. A. & Bacon, D. J. (1997). Raster3D: photorealistic molecular graphics. *Methods Enzymol.* **277**, 505–524.
18. Otwinowski, Z. & Minor, W. (1996). Processing of x-ray diffraction data collected in oscillation mode. *Methods Enzymol.* **276**, 307–325.
19. Kissinger, C. R., Gehlhaar, D. K. & Fogel, D. B. (1999). Rapid automated molecular replacement by evolutionary search. *Acta Crystallog. sect. D*, **55**, 484–491.
20. Jones, T. A., Zou, J. Y., Cowan, S. W. & Kjeldgaard, M. (1991). Improved methods for building protein models in electron-density maps and the location of errors in these models. *Acta Crystallog. sect. A*, **47**, 110–119.
21. Brunger, A. T., Adams, P. D., Clore, G. M., DeLano, W. L., Gros, P., Grosse-Kunstleve, R. W. *et al.* (1998). Crystallography and NMR system: A new software suite for macromolecular structure determination. *Acta Crystallog. sect. D*, **54**, 905–921.
22. Wallace, A. C., Laskowski, R. A. & Thornton, J. M. (1995). Ligplot—a program to generate schematic diagrams of protein ligand interactions. *Protein Eng.* **8**, 127–134.
23. Nicholls, A., Sharp, K. A. & Honig, B. (1991). Protein folding and association—insights from the interfacial and thermodynamic properties of hydrocarbons. *Proteins: Struct. Funct. Genet.* **11**, 281–296.

Edited by R. Huber

(Received 22 January 2003; received in revised form 7 May 2003; accepted 7 May 2003)